On the Balmer Line Problem

K. Werner

Lehrstuhl Astrophysik, Universität Potsdam, Germany

Received ______________________; accepted ______________________

To appear in The Astrophysical Journal Letters

ABSTRACT

The so-called Balmer line problem describes the failure to achieve a consistent fit to the Balmer line spectrum of any hot sdO star whose effective temperature exceeds about 70 000 K. Results of $T_{\rm eff}$ determinations drastically deviate, up to a factor of 2, depending on which Balmer line is examined.

This problem was uncovered a few years ago during non-LTE analyses of very hot subdwarfs and central stars of planetary nebulae. Since then, it cast severe doubt upon non-LTE model atmosphere analysis techniques as a whole. In this Letter we show that the problem is due to the neglect or improper inclusion of metal opacities in the models. On hand of the specific case of BD+28°4211, which is a IUE standard sdO star, we show that the Balmer line problem can be solved when surface cooling by photon escape from the Stark wings of CNO lines is accounted for.

Subject headings: line: formation — radiative transfer — methods: numerical — stars: atmospheres — stars: early-type — stars: fundamental parameters

1. Introduction

As a result of a systematic investigation of the central stars of old, extended planetary nebulae, Napiwotzki (1992) found that the vast majority of them is extremely hot. Subsequent efforts to analyse the Balmer line spectra and to derive effective temperatures failed and led to the discovery of the so-called Balmer line problem. Generally, the fit to the Hα line results in a much lower $T_{\rm eff}$ than the fit to Hδ, while Hβ and Hγ give intermediate values. As an example he showed that the temperature of central star of S 216 amounts to 50 000 K to 90 000 K, depending on which Balmer line, Hα or Hδ, is fitted with synthetic profiles. Independent estimates later indicated that the temperature derived from the highest evaluable Balmer series member (usually Hδ or Hϵ) is giving a realistic result, so that in essence the model atmospheres predict too shallow line profiles for the low series members.

Such drastic discrepancies were later encountered with all analyses of central stars and other hot subdwarfs whose $T_{\rm eff}$ is exceeding 70 000 K, approximately. They cast severe doubts on the reliability of non-LTE model atmospheres, at least in this high-temperature regime, because NLTE model atmospheres composed of hydrogen and helium were the standard tool for this kind of analyses, see e.g. a basic work on central star spectroscopy by Méndez et al. (1988). The Balmer problem is not appearing in that work, because no Balmer line but Hγ is displayed in the profile fits.

We have made several attempts to find the reason for the failure of the NLTE models, without success up to now.

2. Standard Models

Basic NLTE model assumptions are hydrostatic and radiative equilibrium and plane-parallel geometry. Usually, the model atmospheres contain exclusively hydrogen and helium. The reason for this restriction is twofold. First, NLTE model calculations are very costly and metal opacities are time-consuming to deal with. And second, exploratory model calculations accounting for CNO opacities (lines and continua) turned out to have very weak effects on the H and He line profiles (Werner & Heber 1991).

With the advent of a new numerical technique for NLTE model atmosphere calculations, the Accelerated Lambda Iteration method, much more powerful codes became available which overcome the restrictive capacity limits of the original complete linearization technique (Auer & Mihalas 1969). These new codes, independently written by the Kiel/Potsdam and Goddard groups (see Dreizler & Werner 1993, Hubeny 1988, Hubeny & Lanz 1995 for latest developments) allow several numerical approximations to be relaxed which had to be made before. The following, unsuccessful, attempts were made to improve the models and to solve the Balmer line problem.

Metal line blanketing. As already mentioned, the neglect of CNO metals was regarded as a secondary problem. Strong cooling effects due to CNO lines were detected, however, at layers well above the H and He line forming regions. In addition, we could show that the blanketing by millions of lines of the iron group elements has only weak effects on the Balmer lines, too (Dreizler & Werner 1993, Haas et al. 1995).

Line broadening theory. After the inclusion of ion dynamical effects on the theoretical hydrogen Stark profiles by Schöning (1994) there is hardly any doubt now that the broadening theory is in a satisfactory state. He and Napiwotzki & Rauch (1994) showed that the ion dynamical effects are almost negligible for the line formation in hot stars.

Radiation transfer. The simplified treatment of electron scattering of photons as a coherent process was checked and found to be valid in our models.

Electron collisional rates. Effective collision strengths for excitation of hydrogen are still uncertainly known. The accuracy of available data is probably not better than 30% (Pradhan & Gallagher 1992). Numerical experiments show that variation of rates within this range can affect level populations and hence the observed line profiles. Another effect which to our knowledge has not been investigated concerns the neglect of Stark shifts of the level energies when evaluating the collisional rates. While this is easily accounted for in the case of radiative rates by incorporating Stark broadened profiles in the cross sections, there is no simple procedure in the case of collisional rates. Both problems are still unsolved and deserve further attention. In this context it is worth mentioning that the validity of neglecting *proton collisions* has been checked, too. Although the proton collisional rates can exceed the electron collisional rates, this occurs only for transitions between levels with sufficiently high quantum numbers. But the effects are unimportant because electron collisions alone are already very frequent and almost enforce relative LTE populations.

Finally, *sphericity effects* were found to be very small (Kubát 1995) and *wind effects* are likely to be negligible because most of the stars we are concerned here are compact objects.

3. New Models

In order to demonstrate how the Balmer line problem can be solved, we start from a standard model which is thought to represent the sdO star BD+28°4211. It has $T_{\rm eff}$=82 000 K, $\log g$ =6.2, and He/H=0.1. The temperature was confirmed on hand of an independent indicator, the Fe V/Fe VI ionisation balance, which was evaluated from a co-added IUE high-resolution spectrum of outstanding quality (the star is an IUE standard; Haas et al. 1995). The starting model is composed of H and He (represented by 16, 1, 32 NLTE levels for H I, He I, He II, respectively). Line opacities are represented by Doppler profiles, which was a common approximation in earlier NLTE modeling in order to save frequency points. The temperature structure is shown in Fig. 1. It exhibits the characteristic high-temperature plateau in the outer layers ($\log m < -3$) due to heating by H and He II lines, which is a well known feature since the pioneering work of Auer & Mihalas (1969). The corresponding Hα and Hβ line profiles are shown in Fig. 2 and a comparison to spectra from BD+28°4211 is shown in Fig. 3a. The Balmer line problem is evident: The computed lines are too weak. In addition, the central Hα emission core is not reproduced, i.e. not strong enough. Let us now carry out three steps of improvement and discuss their effects on the temperature structure and line profiles as displayed in Figs. 1 and 2.

At first we introduce flux blocking effects by Stark broadened H and He II lines including the Hummer & Mihalas (1988) formalism for level dissolution. For this purpose we used the occupation probability formalism, which was generalized to NLTE conditions by Hubeny et al. (1994). All line profiles become stronger which is a consequence of backwarming effects in deep atmospheric layers and hence increased continuum flux.

In the second step we include the CNO elements (solar abundances). The line opacities are represented by Doppler profiles, like in our previous exploratory calculations (Werner & Heber 1991). As we have expected from that work, the H/He line profiles hardly change (compare short and long-dashed profiles in Fig. 2), although the temperature structure experiences a drastic drop by about 50% at the surface. A high-temperature bump around $\log m = -3$, however, remains. The formation depths of the optical H and He II lines (indicated in Fig. 2) are deep enough to escape the strong surface cooling effects by the CNO lines. Note in passing that the O VI resonance line is extremely optically thick, so that its formation depth ranges from the uppermost layers (Doppler core) down into the continuum forming layers (Stark wings).

In the final step Stark broadening instead of Doppler broadening for the CNO lines is introduced. Stark profiles are computed in an approximate manner as described in detail by Werner et al. (1991). Further backwarming effects are negligible but the high-temperature bump completely disappears! Cooling by up to 15 000 K occurs by photon escape from the broad C IV, N V, O VI Stark line wings, resulting in a strictly monotonous run of the temperature with depth. As a result the line cores of Hβ and Hγ, which are now affected by the cooling process, get deeper and almost match the observation. For the same reason the Hα NLTE emission core is strongly increased and now perfectly coincides with the observed peak height (Fig. 3a). The reason for this surprising behaviour of Hα is twofold. The drop of the local temperature in the line core forming region increases NLTE effects because of the enlarged difference between the (non-local) radiation field formed in deep layers and the local Planck value. On the other hand the source function in the line center is increased by a decrease of the n=2 departure coefficient. In an analogous study of iron line blanketing effects, this was traced back to a decrease in the photoionisation rate in the Balmer continuum, due to surface cooling and direct metal line blocking (Lanz & Hubeny 1995).

It is interesting to note, that the temperature structure of our best NLTE model is also that one which most closely resembles the LTE model.

4. Conclusion

Several improvements in the NLTE models result in a Balmer line fit to BD+28°4211 which is much closer to the observation than before. Of most serious consequences is the cooling through the Stark wings of broadened CNO lines. Experience shows, that not only the resonance line series are to be treated realistically, but equally important are line series from excited levels. Another example is displayed in Fig. 3b. It shows the spectrum of the central star of S 216, with which the Balmer line problem was first demonstrated. Like in Fig. 3a (BD+28°4211) we compare it with two models, a simple H/He model which gives much too weak Hα–Hγ lines, and a model accounting for Stark broadened CNO profiles, which gives an almost perfect fit.

In essence we conclude that the Balmer line problem disappears when metal line opacities are included in a realistic manner. Since higher Balmer series members than Hδ are almost unaffected by the neglect of CNO opacities, we can confirm the suspicion of Napiwotzki & Schönberner (1993) that relying on these lines gives a realistic $T_{\rm eff}$ determination.

Close inspection of our best fit model (Fig. 3a) reveals that the computed lines are still slightly too weak. It is reasonable to assume that the additional inclusion of all other metals heavier than CNO up to the iron group will remove the remaining discrepancy. This step is probably more important in even hotter stars, since preliminary calculations show that the remaining discrepancies are larger there than in BD+28°4211 and S 216. Corresponding calculations are being prepared, though the task is rather difficult. The model calculations presented here involve more than 170 non-LTE levels and 8000 frequency points and require considerable amounts of computer time.

A DFG grant (We 1312/6-1) is gratefully acknowledged. Computations were performed on Cray computers of the Rechenzentrum der Universität Kiel.

REFERENCES

Auer, L.H., & Mihalas, D. 1969, ApJ, 158, 641

Dreizler, S., & Werner, K. 1993, A&A, 278, 199

Haas, S., Dreizler, S., Heber, U., Jeffery, S., & Werner, K. 1995, A&A, in press

Hubeny, I. 1988, Comput. Phys. Commun., 52, 103

Hubeny, I., & Lanz, T. 1995, ApJ, 439, 875

Hubeny, I., Hummer, D.G., & Lanz, T. 1994, A&A, 282, 157

Hummer, D.G., & Mihalas, D. 1988, ApJ, 331, 794

Kubát, J. 1995, A&A, 299, 803

Lanz, T., & Hubeny, I. 1995, ApJ, 439, 905

Méndez, R.H., Kudritzki, R.P., Herrero, A., Husfeld, D., & Groth, H.G. 1988, A&A, 190, 113

Napiwotzki, R. 1992, in The Atmospheres of Early Type Stars, Lecture Notes in Physics, Vol. 401, ed. U. Heber, & C.S. Jeffery (Berlin: Springer), 310

Napiwotzki, R., & Schönberner, D. 1993, in White Dwarfs: Advances in Observation and Theory, NATO ASI Series C, Vol. 403, ed. M. Barstow (Dordrecht: Kluwer), 99

Napiwotzki, R., & Rauch, T. 1994, A&A, 285, 603

Pradhan, A.K., & Gallagher, J.W. 1992, Atomic Data And Nuclear Data Tables, 52, 227

Schöning, T. 1994, A&A, 282, 994

Werner, K., & Heber, U. 1991, in Stellar Atmospheres: Beyond Classical Models, NATO ASI Series C, Vol. 341, ed. L. Crivellari, I. Hubeny, & D.G. Hummer (Dordrecht: Kluwer), 341

Werner, K., Heber, U., & Hunger, K. 1991, A&A, 244, 437

Fig. 1.— Temperature structures of four non-LTE model atmospheres with increasing degree of sophistication as discussed in the text. A LTE model is shown for comparison (triangles). While pure H-He models show a high-temperature plateau at the surface, our most sophisticated model shows a monotonous temperature run (full line). Formation depth intervals for selected lines are represented by horizontal bars. The Hα and Hβ line profiles of the four non-LTE models are compared in Fig. 2. Model parameters are $T_{\rm eff}$=82 000 K, $\log g$ =6.2, and solar abundance ratios.

Fig. 2.— Hα and Hβ line profiles of the four non-LTE models which were shown in Fig. 1. Generally, with increasing degree of model sophistication the lines become deeper while the Hα emission core increases considerably. All profiles were folded with a 1.5Å FWHM Gaussian.

Fig. 3.— a) Line profile fits to BD+28°4211 (left panel) and b) to the central star of S 216 (right panel). Two sets of synthetic profiles are plotted, namely that from the pure H-He model (Doppler profiles, dashed) and that from the model with CNO and Stark broadened profiles. The Balmer line problem is occurring with the former set and essentially disappears with the latter. Computed profiles are folded with appropriate Gaussians to match the instrumental resolution. Model parameters for BD+28°4211 like in Fig. 1, for S 216: $T_{\rm eff}$=85 000 K, $\log g$ =6.9, CNO solar, He/H=0.06.

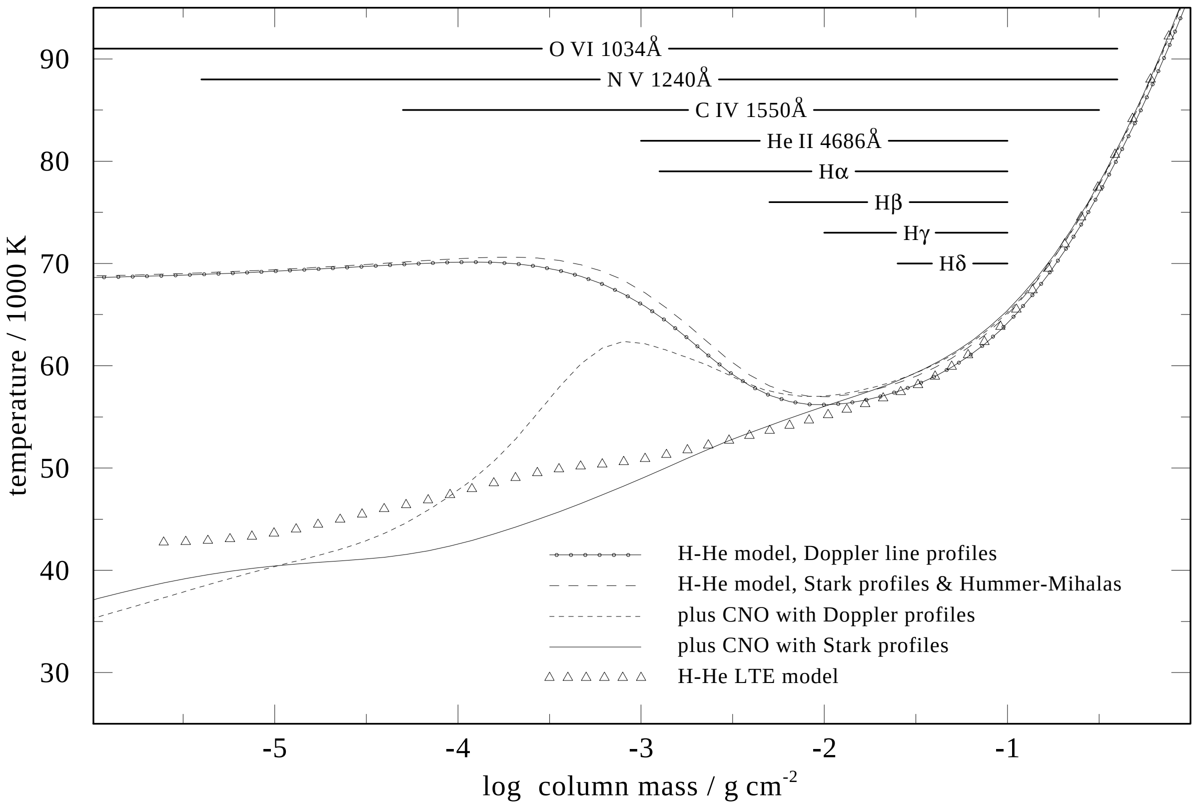
O VI 1034Å
N V 1240Å
C IV 1550Å
He II 4686Å
Hα
Hβ
Hγ
Hδ
90
80
70
60
50
40
30
temperature / 1000 K
-5
-4
-3
-2
-1
log column mass / g cm-2
H-He model, Doppler line profiles
H-He model, Stark profiles & Hummer-Mihalas
plus CNO with Doppler profiles
plus CNO with Stark profiles
H-He LTE model

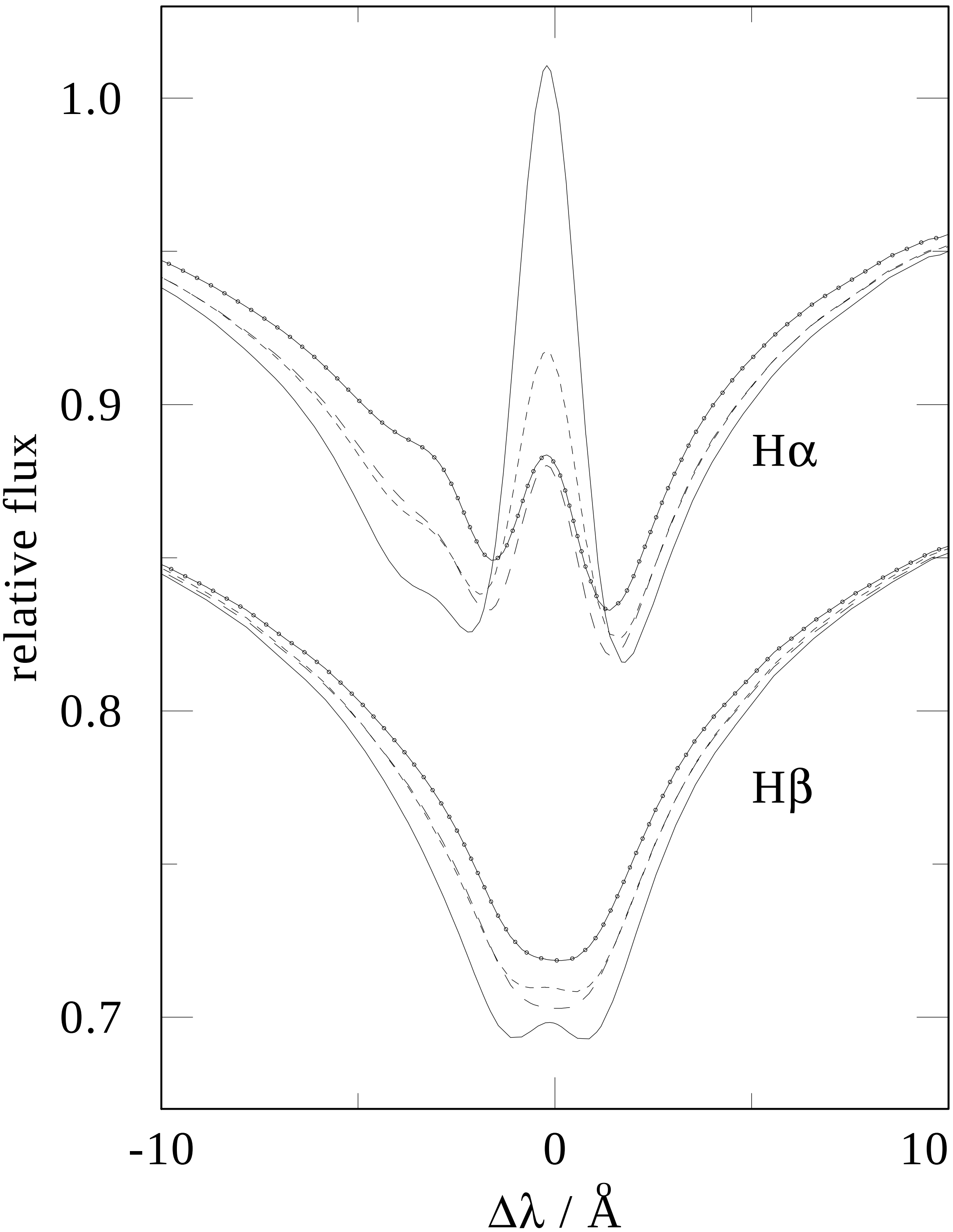
1.0
0.9
0.8
0.7
relative flux
Hα
Hβ
-10
0
10
Δλ / Å

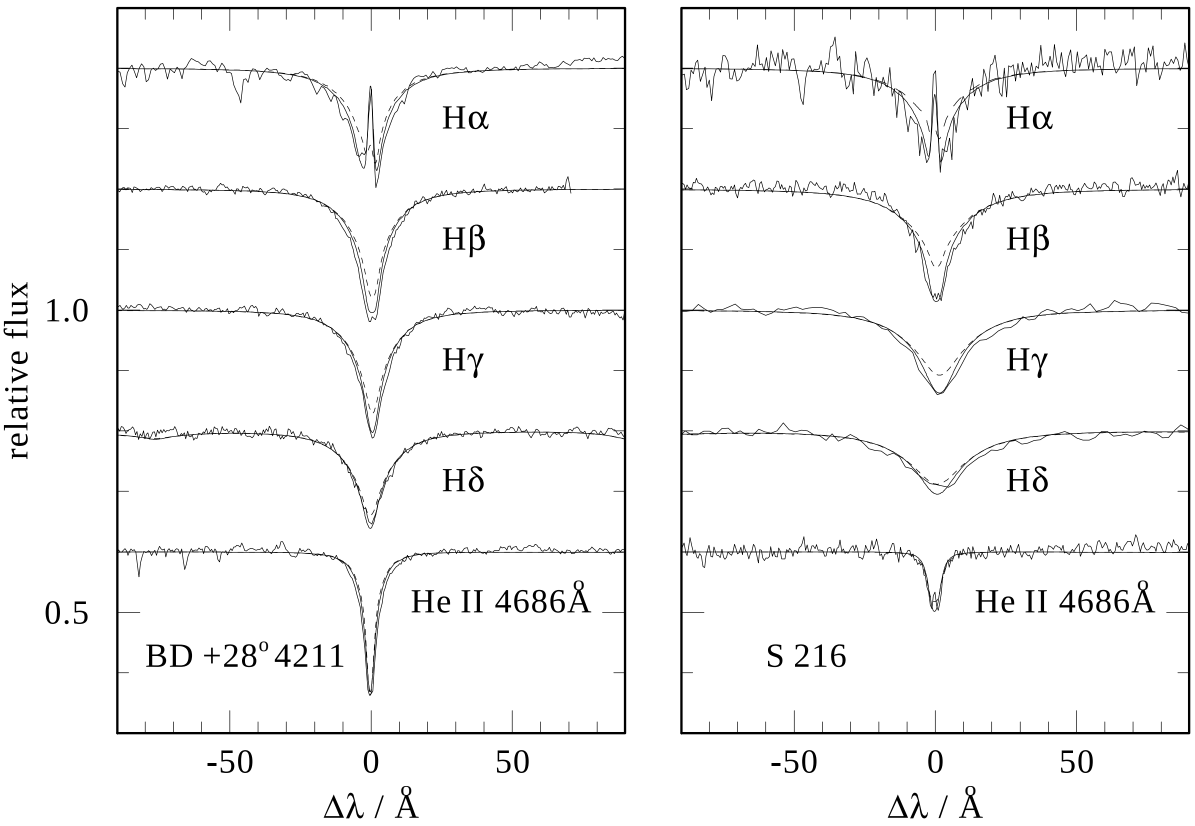
relative flux
1.0
0.5
Hα
Hβ
Hγ
Hδ
He II 4686Å
BD +28° 4211
-50
0
50
Δλ / Å
Hα
Hβ
Hγ
Hδ
He II 4686Å
S 216
-50
0
50
Δλ / Å